Starting-point-independent quantum Monte Carlo calculations of iron oxide

Joshua P. Townsend [1,*] Sergio D. Pineda Flores,[2] Raymond C. Clay, III,[1] Thomas R. Mattsson,[1] Eric Neuscamman [2]
Luning Zhao [3] R. E. Cohen,[4] and Luke Shulenburger[1]

[1]*High Energy Density Physics Theory, Sandia National Laboratories, Albuquerque, New Mexico 87185, USA*
[2]*Department of Chemistry, University of California, Berkeley, California 94720, USA*
[3]*Department of Chemistry, University of Washington, Seattle, Washington 98195, USA*
[4]*Extreme Materials Initiative, Earth and Planets Laboratory, Carnegie Institution for Science, Washington DC 20015-1305, USA*

Quantum Monte Carlo (QMC) methods are useful for studies of strongly correlated materials because they are many body in nature and use the physical Hamiltonian. Typical calculations assume as a starting point a wave function constructed from single-particle orbitals obtained from one-body methods, e.g., density functional theory. However, mean-field-derived wave functions can sometimes lead to systematic QMC biases if the mean-field result poorly describes the true ground state. Here, we study the accuracy and flexibility of QMC trial wave functions using variational and fixed-node diffusion QMC estimates of the total spin density and lattice distortion of antiferromagnetic iron oxide (FeO) in the ground state $B1$ crystal structure. We found that for relatively simple wave functions the predicted lattice distortion was controlled by the choice of single-particle orbitals used to construct the wave function, rather than by subsequent wave function optimization techniques within QMC. By optimizing the orbitals with QMC, we then demonstrate starting-point independence of the trial wave function with respect to the method by which the orbitals were constructed by demonstrating convergence of the energy, spin density, and predicted lattice distortion for two qualitatively different sets of orbitals. The results suggest that orbital optimization is a promising method for accurate many-body calculations of strongly correlated condensed phases.

I. INTRODUCTION

Iron oxide (wüstite, FeO) is a prototypical charge transfer insulator which displays a rich phase diagram that includes magnetic, electronic, and structural phase transformations due in part to the open-shell configuration of the $3d$ electrons [1–8]. In the ground state, FeO adopts a bulk antiferromagnetic (AFM) structure composed of alternating ferromagnetic planes of Fe atoms perpendicular to [111] which induces a symmetry-lowering distortion of the nominally cubic $B1$ lattice [9,10]. Previous theoretical studies have investigated structural phase transitions at high pressure and the equilibrium lattice distortion [8,11–19]. One of the main findings of these studies is that the predicted lattice distortion is particularly sensitive to the treatment of the electrons.

Quantum Monte Carlo (QMC) methods are especially well suited to problems where electronic correlation is important because they use the physical Hamiltonian and are therefore variational [20,21]. The input for a typical QMC calculation is a trial wave function, the antisymmetric portion of which is often generated from a set of single-particle orbitals (SPOs) from mean-field methods such as Kohn-Sham density functional theory (DFT). In addition to the antisymmetric piece, the trial wave function typically includes many adjustable parameters which can be optimized by exploiting the

variational principle using, for example, variational Monte Carlo (VMC). Classic examples include the Jastrow factor, backflow transformation of the electronic coordinates, a multideterminant expansion, and orbital optimization. Each of the above has been studied extensively in atomic, molecular, and condensed regimes because such wave functions explicitly introduce electron-electron correlation into the wave function and thereby give improved ground-state properties compared to a mean-field wave function [22–28].

Complementary to VMC is diffusion Monte Carlo (DMC), a projector-based method whose accuracy depends on the nodal surface of the wave function, which in turn depends on the SPO set. The challenge for highly accurate QMC studies of strongly correlated systems, then, lies in constructing a suitably flexible wave function which can repair any deficiencies inherited from the mean-field SPOs. Thus new methods for generating accurate QMC trial wave functions with sufficient flexibility are highly desired. Several previous studies have demonstrated remarkable success in constructing flexible and accurate wave functions in atomic and molecular systems [22,26,29–32], but until now wave functions for condensed systems have tended to be much simpler due to the larger number of electrons and larger basis sets.

Here we report variational and diffusion quantum Monte Carlo calculations of AFM FeO using a variety of trial wave function *Ansätze*, including electron-electron backflow transformations as well as multideterminant expansions and orbital optimization. In order to test the flexibility of the trial wave

*jptowns@sandia.gov

function, we constructed two sets of DFT SPOs using Perdew-Burke-Ernzerhof (PBE) and PBE + U functionals generated to yield qualitatively different lattice distortions and spin densities. We then demonstrate the starting-point independence of DMC estimates of the energy, spin density, and equilibrium lattice distortion with respect to the SPOs in a Slater Jastrow wave function through orbital optimization and show that this was not possible for either backflow or small multideterminant wave functions. The results indicate that orbital optimization is a promising method for constructing very accurate and flexible wave functions for QMC calculations in systems where mean-field descriptions yield an incorrect ground state and highlight the potential of QMC methods to deliver starting-point-independent estimates of some ground-state properties in strongly correlated condensed phases.

II. COMPUTATIONAL APPROACH

The immediate goal of this study was to understand how the techniques used to construct QMC trial wave functions affected the estimated ground-state properties in a challenging condensed system. With that goal in mind, we restricted calculations to a single four-atom AFM primitive cell so that advanced wave function *Ansätze* which scale unfavorably with system size could be tested.

The building block of all the trial wave functions considered here was the Slater-Jastrow (SJ)-type wave function:

$$\Psi_T(\mathbf{r}; \alpha, \beta) = D^{\uparrow}(\mathbf{r}; \alpha) D^{\downarrow}(\mathbf{r}; \alpha) e^{J(\mathbf{r}; \beta)}, \qquad (1)$$

where $\mathbf{r}$ is the set of electronic coordinates, $\{\alpha, \beta\}$ are the set of variational parameters, and $D^{\uparrow,\downarrow}$ is a Slater determinant composed of SPOs. The adjustable parameters α of the antisymmetric portion of the wave function include, for example, weights in a multideterminant expansion, electron-electron backflow transformation, and orbital rotations. Finally, $J(\mathbf{r}; \beta)$ is the Jastrow function that explicitly introduces dynamic correlation into the wave function and enforces the cusp conditions [23,33,34].

The DMC algorithm applied to fermions commonly requires that the nodal surface $[\Psi_T(\mathbf{r}; \alpha, \beta) = 0]$ of the trial wave function is prescribed in order to mitigate the fermion sign problem [35,36]. This fixed-node approximation introduces a systematic bias in the results, which, while variational, may be significant if the nodal surface of the trial wave function is qualitatively different from that of the exact ground-state wave function. As we show later, this bias can sometimes result in qualitatively incorrect behavior even after wave function optimization.

A. Wave function generation

In order to test the flexibility of QMC trial wave functions we constructed two sets of SPOs which produced qualitatively different estimates of the spin density and equilibrium lattice distortion. Trial wave functions were constructed from SPOs generated from spin-unrestricted DFT calculations using the QUANTUM ESPRESSO code (version 6.4.0), an implementation of plane-wave-based Kohn-Sham density functional theory with periodic boundary conditions [37]. We used pseudopotentials specifically designed for QMC calculations to

describe the iron and oxygen atoms for both the DFT and QMC calculations [38]. The iron pseudopotential had a neon core ($3s^2 3p^6 3d^6 4s^2$ valence), and the oxygen pseudopotential had a helium core ($2s^2 2p^4$ valence), for a total of 44 electrons in the primitive cell. All DFT calculations used a 180-hartree plane wave cutoff and a $6 \times 6 \times 6$ k-point grid and were tested to confirm that further increasing those values did not appreciably change the DFT energy or stress. The first SPO set was constructed using the PBE generalized gradient approximation [39], and the second used a PBE+U functional ($U = 4.3$ eV) in the rotationally invariant scheme following previous work [16,17] in order to localize the Fe 3d states. The two sets of SPOs are qualitatively distinct and essentially describe two different materials. The PBE result predicted a metallic ground state and a positive lattice distortion, while the PBE + U results predicted an insulating ground state and negative lattice distortion.

B. Wave function optimization and Monte Carlo calculations

All QMC calculations were performed with the QMCPACK code (version 3.6) [40]. We used the improved adaptive shift algorithm [41] to optimize, in some cases, more than 3000 wave function parameters using VMC. Common among all trial wave functions we considered were species-dependent one-, two-, and three-body Jastrow factors represented as cubic polynomials in the particle separations with a spatial cutoff corresponding to the Wigner-Seitz radius of the cell, about 2.9 bohrs. The two-body Jastrow produced the largest energy and variance reduction, but the addition of one- and three-body terms was found to further reduce the energy and variance significantly. The use of small core pseudopotentials resulted in a highly oscillatory wave function near the atomic cores which was costly in terms of memory to accurately represent on a rectangular mesh. We therefore chose to divide the representation of the wave function into two parts, as suggested by Esler *et al.* [42], with the regions near the ions stored as radial splines multiplied by spherical harmonics and the interstitial regions represented by three-dimensional B splines on a rectilinear mesh [43]. This scheme reduced the memory required to represent the wave function by a factor of more than 25 compared to the standard rectangular mesh with no statistically significant change in the energy or variance.

With two sets of SPOs in hand, we proceeded to optimize the trial wave functions using VMC. While optimization of the Jastrow factor yielded significant energy and variance reduction, the SPOs themselves are what limit the ultimate accuracy of DMC. We therefore explored three methods of improving the nodal surface of the trial wave function: backflow transformation of the electronic coordinates, multideterminant expansion, and orbital optimization. A backflow (BF) transformation is a transformation of the electronic coordinates $\mathbf{r}$ to quasiparticle coordinates $\mathbf{q}$ [44]. For a particular electron this transformation is given by

$$\mathbf{r}_i \rightarrow \mathbf{q}_i = \mathbf{r}_i + \sum_j \eta(|\mathbf{r}_i - \mathbf{r}_j|; \alpha)(\mathbf{r}_i - \mathbf{r}_j), \qquad (2)$$

with η being a spherically symmetric cubic spline function.

The second trial wave function type was a multideterminant (MD) expansion. In this wave function, one builds out

of a set of single-particle orbitals $\{\phi\}$ and a number of Slater determinants $\{\Phi[\phi]\}$, with the former being larger than the number of electrons per spin channel:

$$D(\mathbf{r}, \alpha) = \sum_i \alpha_i \Phi_i[\phi(\mathbf{r})]. \qquad (3)$$

The appeal of this *Ansatz* is that with an infinite number of ϕ's and Φ's, this wave function is exact. Unfortunately, it scales exponentially in the number of particles. For that reason, we explored the use of modest multideterminant expansions which were constructed in a two-step procedure. The first step was a VMC optimization of the 924 determinant weights in an expansion consisting of all possible single excitations within a basis of 64 SPOs. The second step was a VMC optimization of all possible single and double excitations generated from the highest weighted 32 determinants from the previous step, which totaled 452 determinants. For these wave functions we found that optimization of the weights of the determinants at each twist further reduced the VMC energy by approximately 20 mhartree/FeO compared to optimization at only a single twist due to differences in orbital energy ordering.

The third trial wave function type included an optimization of the SPOs (OO) themselves. With this method, each optimized SPO $\tilde{\phi}$ present in the determinant is constructed from a unitary transformation of the original SPOs ϕ [26–29]:

$$\tilde{\phi}_i = \sum_j \alpha_{ij} \phi_j. \qquad (4)$$

This wave function contained over 3000 optimizable parameters and was therefore expected to be the most flexible and accurate trial wave function type we considered.

After optimization, production DMC calculations were carried out on all optimized trial wave functions on a $3 \times 3 \times 3$ grid of twist vectors, and the results were subsequently twist averaged. DMC results were linearly extrapolated to zero time step from a series of calculations with finite time steps of $\tau = 0.01$, 0.005, and 0.0025 hartree^{-1}.

III. RESULTS

The principal goal of this study was to understand how sensitive various ground-state properties of a system were to the trial wave function for a realistic and challenging condensed system. To that end, we calculated a series of physical properties that are typically strongly affected by the electronic structure: the total spin density and the equilibrium lattice distortion.

We compare the twist-averaged total energies for all optimized trial wave functions for an undistorted (cubic) geometry in Fig. 1. As expected, the VMC energies of the optimized backflow, multideterminant, and orbital optimization wave functions were lower than their simpler Slater-Jastrow wave function counterparts. An unexpected result was that improvements in the multideterminant trial wave function predicted by VMC did not carry over to DMC in all cases. We attribute this result to the relatively small active space in which that wave function was constructed, and it suggests that our VMC optimization strategy improves the overall shape of the wave function but not necessarily its nodal surface. Importantly, the DMC energies of the orbital optimized trial wave function
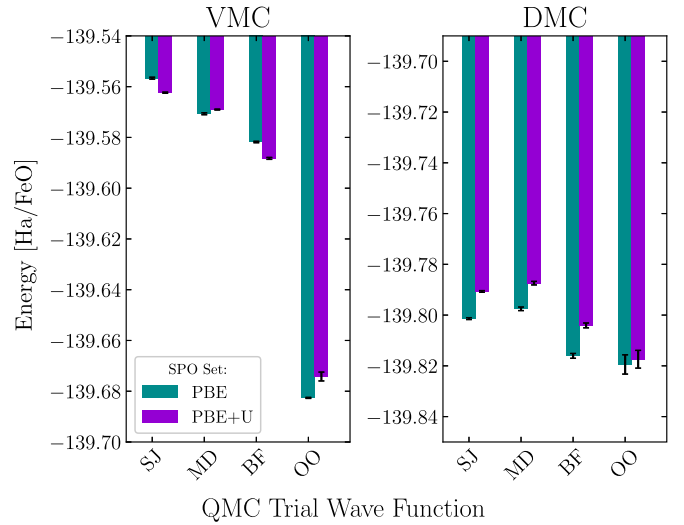

FIG. 1. Twist-averaged QMC energies for several optimized trial wave function types built from either PBE or PBE+U SPOs. The DMC energies are linearly extrapolated to zero time step. Abbreviations: SJ = Slater Jastrow, MD = multi determinant, BF = backflow, and OO = orbital optimization.

were statistically identical regardless of the SPO set in which the optimization occurred, a result unique to this wave function. Especially encouraging was that the OO wave function was much less expensive to evaluate than the MD or BF, which were 2.2 and 1.6 times as expensive to evaluate as the OO wave function, respectively.

A. Spin density

The character of the Fe $3d$ orbitals produced from our PBE $+ U$ calculations is very different from those of PBE. As a result, we expected to see a significant difference in the predicted total spin densities depending on the SPOs used in the trial wave function. An open question was how significantly the spin density would change after optimization. To illustrate the differences in the spin densities obtained from the optimized trial wave functions, we show differences in the DMC estimates from various wave functions with respect to that from a single-determinant SJ wave function composed of PBE SPOs in Fig. 2. Because estimates of observables from different wave functions are subject to different time step errors, all DMC results have been linearly extrapolated to zero time step. Additionally, the spin density estimator does not commute with the Hamiltonian, which means that our DMC spin densities were subject to a mixed estimator bias, which we have corrected [36]. While both the backflow and multideterminant trial wave functions show only small perturbations in the spin density compared to the SJ PBE reference (comparing the top and bottom rows of Fig. 2, excluding the rightmost illustrations), the orbital optimized trial wave function yields a significantly different spin density (rightmost illustrations of Fig. 2). Significantly, the qualitatively distinct characters of the PBE and PBE $+ U$ SPOs are effectively erased with orbital optimization (top and bottom rightmost illustrations in Fig. 2). In concordance with the comparison of the total energy shown in Fig. 1, the convergence of the
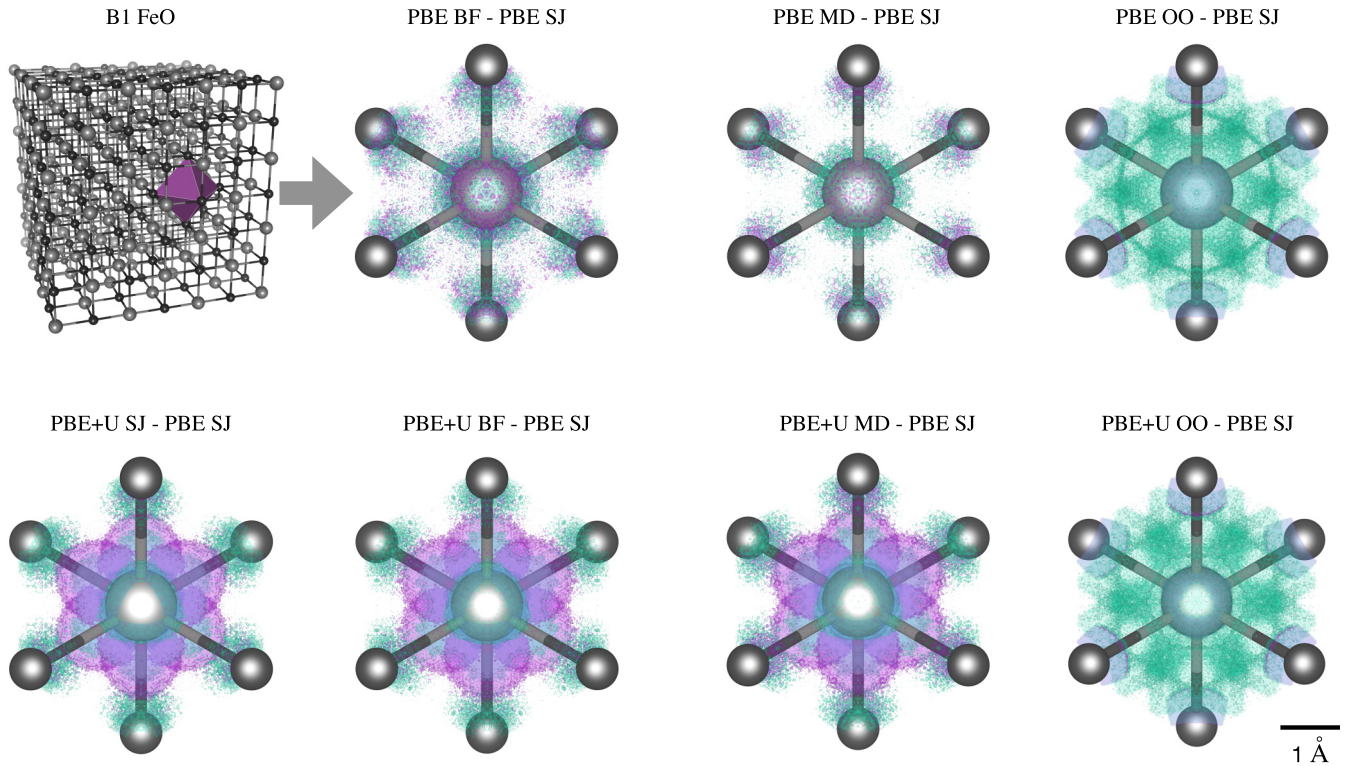
FIG. 2. Differences in the DMC estimated total spin density between trial wave function types with respect to a single SJ trial wave function composed of PBE SPOs. Detailed views looking along [111] show an isosurface corresponding to 2% of the maximum difference and are restricted to a single FeO_6 octahedron for visual clarity. Iron and oxygen atoms are shown as large gray and small black spheres, respectively. Green (purple) surfaces bound regions where PBE total spin density is less (greater) than that from the other SPO set.

spin density suggests that the observables computed from the orbitally optimized wave function were independent of the underlying SPO set.

B. Equilibrium lattice distortion

In the ground state, the nominally cubic $B1$ crystal structure of AFM FeO is slightly elongated along the [111] direction, thereby simultaneously increasing the interplanar spacing and decreasing the intraplanar spacing of the iron atoms [45,46]. This phenomenon is observed in many transition metal oxides and is controlled by interactions between $3d$ electrons on the iron atoms [47,48]. For that reason we expected the equilibrium lattice distortion to be very sensitive to the quality of the trial wave function. Figure 3 shows energy versus lattice distortion at the VMC and DMC levels. The VMC results for each wave function type universally predicted lattice contraction along [111], which is qualitatively wrong compared to experiment.

Considering the more accurate DMC calculations, we see significant improvements in both energy and predicted lattice distortion. DMC correctly shifted the predicted equilibrium lattice distortion for all trial wave functions to more positive values (corresponding to extension along [111]), although this shift is insufficient to recover the correct behavior in some cases. There was also a reordering of the relative energies of the trial wave functions compared to VMC. Wave functions constructed from PBE+U orbitals yielded higher DMC en-

ergies compared to those of the PBE wave functions. That the multideterminant wave functions produce a higher energy than their single-determinant counterparts at the DMC level is a reflection of the fact that wave function improvements from VMC do not necessarily guarantee a corresponding improvement with DMC but could probably be improved via a larger multideterminant expansion [29]. Compared to the multideterminant expansion, the improvements in the nodal surface due to the backflow transformation and orbital optimization are readily apparent both in terms of lower total energy and lattice distortion. Indeed, the backflow and orbital optimized wave functions yielded significant energy reductions, in some cases reducing the energy by as much as 20 mhartree per FeO compared to the single SJ trial wave function. Overall, we found that the orbital optimized wave function produced the lowest VMC and DMC total energies, which indicates that it was the most accurate wave function among those tested.

As expected, the predicted equilibrium distortion is quite sensitive to the trial wave function. For example, a SJ trial wave function composed of PBE orbitals predicts an equilibrium distortion of about 1.9%, while the backflow and multideterminant wave functions predicted 2.0% and 2.4%, respectively. By design, we constructed the PBE + U wave function in such a way to accumulate excess charge between Fe atoms along [111] compared to the other wave functions, which explains why the PBE + U wave function uniquely predicted a negative lattice distortion at the DMC level. Estimates of the distortion from trial wave functions
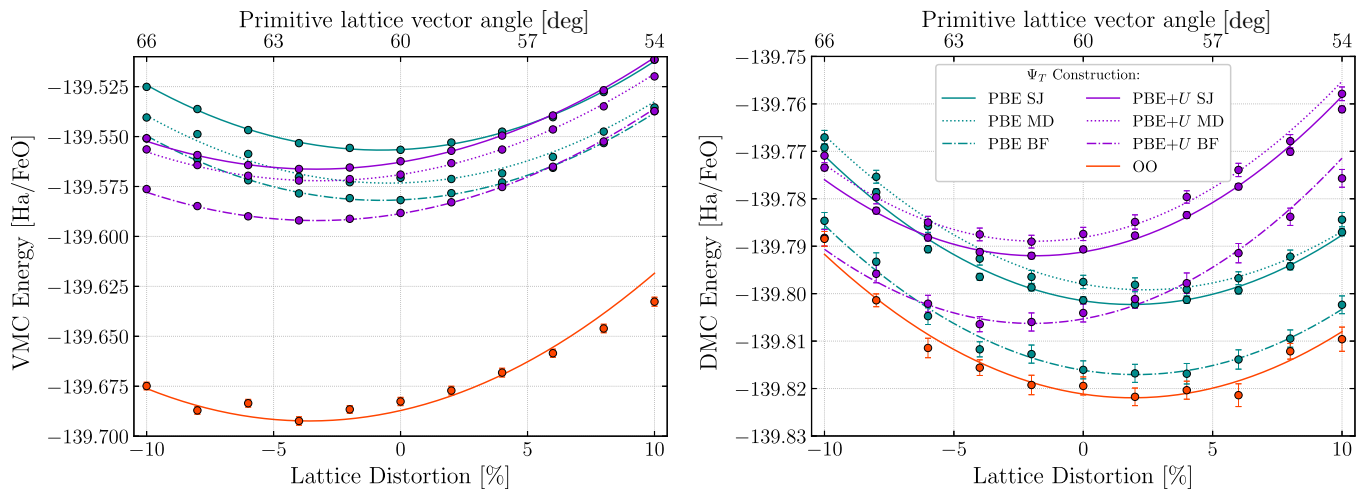
FIG. 3. Energy versus lattice distortion for VMC (left) and DMC (right) calculations with trial wave functions constructed from various DFT-based methods. The solid lines are quadratic polynomial fits to the data and are included as a guide to the eye.

composed of PBE $+ U$ SPOs show remarkably little variation in the predicted lattice distortion. We found standard SJ, backflow, and multideterminant estimates of -1.8%, -2.0%, and -1.8%, respectively. Finally, the estimated distortion from the orbital optimization wave function was 1.9%. For FeO, comparison to experiment is hampered by the fact that natural and synthetic samples are nonstoichiometric. Nevertheless, experimental measurements suggest lattice distortion between about 1% and 2% [10,45,46]. Admittedly, the large uncertainty in the experimental data, likely due in part to stoichiometry, is consistent with several of our QMC estimates. However, in terms of the present study, the low energy of the orbital optimization trial wave function suggests that it is the most accurate.

IV. DISCUSSION AND CONCLUSIONS

The goal of this study was to understand how the SPOs used to construct the QMC trial wave function affected several ground-state properties and to test the extent to which various QMC wave functions provided estimates of observables that were independent of the quality of the SPOs. The most significant result of this investigation was the demonstration of the starting-point independence of the QMC trial wave function with respect to the energy, spin density, and predicted lattice distortion via orbital optimization, which was not achieved using any other wave functions that we considered. This suggests that wave functions of this form may provide truly *ab initio* QMC estimates of ground-state properties for materials in which a mean-field description sometimes gives incorrect results.

The results presented here are subject to several limitations. Most importantly, the 44-electron, 4-atom primitive cell considered here is too small to make meaningful estimates of observables in the thermodynamic limit. This limitation was unavoidable in order to explore advanced wave functions which scale unfavorably with system size. Given the small simulation cell, it is reasonable to question how much of what

we have observed will carry over to the thermodynamic limit. What this work shows is that there are qualitative differences and large quantitative energy differences in the underlying orbitals and charge distributions between various flavors of mean-field DFT and VMC orbital optimization, most notably on the iron site. If we consider a mapping of our FeO primitive cell onto a Hubbard model, it would imply notable changes to the nearest-neighbor and interband hopping and on-site Coulomb repulsion integrals. It seems to us that short of a coincidence whereby PBE, PBE $+ U$, and subsequent VMC orbital optimization all give similar orbitals in the thermodynamic limit, the issues identified in this work will also arise in larger systems and will require similar mitigation strategies to what we have demonstrated here.

Beyond issues of simulation size, the ground-state wave function of an antiferromagnet is, in general, not a single Slater determinant. To understand how the restriction on the wave function *Ansatz* affects the present results, we ask what the variational improvement in energy could be from a better treatment of magnetic degrees of freedom. By comparing QMC energy estimates for single-reference versus resonating valence bond type wave functions for antiferromagnetic ground states in the two-dimensional Heisenberg model with an effective J of the order of 1 eV, we can estimate that the relevant magnetic energy scale in FeO is about 1 mhartree per formula unit [49]. In contrast, we found that the energy scale coming from changes in the mean-field orbitals was of the order of 10 mhartree/f.u. for DMC and of the order of 50 mhartree/f.u. for VMC (Fig. 1). This suggests that whether one has the right magnetic ground state is of secondary importance in modeling these systems (in terms of their energy) compared to the shape of the orbitals and overall charge distributions. In the present study, we cannot claim to have the correct ground state of FeO; however, this work does show that orbital optimization is a promising first step in the construction of more sophisticated *Ansätze* for QMC investigations of magnetic systems. Finally, we emphasize that within DFT or DFT+U there are multiple minima with different symmetries

and geometries. The ground state is monoclinic [16,50]. Even local spin density approximation (LSDA) gives the correct positive strain [11] and LDA clearly shows minima for both positive and negative strains. Recently it is also shown that the SCAN functional gives the correct ground state and a gap even for the disordered paramagnetic state [50].

In conclusion, we have performed a systematic investigation of some ground-state properties of AFM *B*1 FeO, and in particular we explored several QMC wave function generation techniques. The results suggest that the equilibrium lattice distortion and spin density are exceptionally sensitive to the construction of the trial wave function (viz., the nodal surface). We demonstrated the starting-point independence of the QMC trial wave function with respect to the energy, spin density, and equilibrium lattice distortion through orbital optimization. Finally, we suggest that advanced and systematically improvable QMC wave functions achieved via orbital optimization may soon be used more extensively in condensed-matter systems for problems where strong electronic correlation effects are important.

Input files used in this study can be found at Ref. [51].

[1] D. Adler, Rev. Mod. Phys. **40**, 714 (1968).

[2] N. Mott, *Metal-Insulator Transitions* (Taylor and Francis, London, UK, 1974).

[3] M. P. Pasternak, R. D. Taylor, R. Jeanloz, X. Li, J. H. Nguyen, and C. A. McCammon, Phys. Rev. Lett. **79**, 5046 (1997).

[4] J. Badro, V. V. Struzhkin, J. Shu, R. J. Hemley, H.-k. Mao, C.-c. Kao, J.-P. Rueff, and G. Shen, Phys. Rev. Lett. **83**, 4101 (1999).

[5] S. Ono, Y. Ohishi, and T. Kikegawa, J. Phys.: Condens. Matter **19**, 036205 (2007).

[6] A. O. Shorikov, Z. V. Pchelkina, V. I. Anisimov, S. L. Skornyakov, and M. A. Korotin, Phys. Rev. B **82**, 195101 (2010).

[7] R. A. Fischer, A. J. Campbell, G. A. Shofner, O. T. Lord, P. Dera, and V. B. Prakapenka, Earth Planet. Sci. Lett. **304**, 496 (2011).

[8] K. Ohta, R. E. Cohen, K. Hirose, K. Haule, K. Shimizu, and Y. Ohishi, Phys. Rev. Lett. **108**, 026403 (2012).

[9] C. Shull, W. Strauser, and E. Wollan, Phys. Rev. **83**, 333 (1951).

[10] B. T. M. Willis and H. P. Rooksby, Acta Crystallogr. **6**, 827 (1953).

[11] D. G. Isaak, R. E. Cohen, M. J. Mehl, and D. J. Singh, Phys. Rev. B **47**, 7720 (1993).

[12] R. E. Cohen, I. I. Mazin, and D. G. Isaak, Science **275**, 654 (1997).

[13] I. I. Mazin, Y. Fei, R. Downs, and R. E. Cohen, Am. Mineral. **83**, 451 (1998).

[14] Z. Fang, K. Terakura, H. Sawada, T. Miyazaki, and I. Solovyev, Phys. Rev. Lett. **81**, 1027 (1998).

[15] Z. Fang, I. V. Solovyev, H. Sawada, and K. Terakura, Phys. Rev. B **59**, 762 (1999).

[16] S. A. Gramsch, R. E. Cohen, and S. Y. Savrasov, Am. Mineral. **88**, 257 (2003).

[17] M. Cococcioni and S. de Gironcoli, Phys. Rev. B **71**, 035105 (2005).

[18] J. Kolorenč and L. Mitas, Phys. Rev. Lett. **101**, 185502 (2008).

[19] J. Kolorenč, S. Hu, and L. Mitas, Phys. Rev. B **82**, 115108 (2010).

[20] W. M. C. Foulkes, L. Mitas, R. J. Needs, and G. Rajagopal, Rev. Mod. Phys. **73**, 33 (2001).

[21] R. Needs, M. Towler, N. Drummond, and P. L. Ríos, J. Phys.: Condens. Matter **22**, 023201 (2010).

[22] C. Filippi and S. Fahy, J. Chem. Phys. **112**, 3523 (2000).

[23] N. D. Drummond, M. D. Towler, and R. J. Needs, Phys. Rev. B **70**, 235119 (2004).

[24] P. López Ríos, A. Ma, N. D. Drummond, M. D. Towler, and R. J. Needs, Phys. Rev. E **74**, 066701 (2006).

[25] C. J. Umrigar, J. Toulouse, C. Filippi, S. Sorella, and R. G. Hennig, Phys. Rev. Lett. **98**, 110201 (2007).

[26] J. Toulouse and C. J. Umrigar, J. Chem. Phys. **128**, 174101 (2008).

[27] T. Helgaker, P. Jorgensen, and J. Olsen, *Molecular Electronic-Structure Theory* (Wiley, Hoboken, NJ, 2014).

[28] S. Pathak and L. K. Wagner, J. Chem. Phys. **149**, 234104 (2018).

[29] E. Giner, R. Assaraf, and J. Toulouse, Mol. Phys. **114**, 910 (2016).

[30] J. Ludovicy, K. H. Mood, and A. Lüchow, J. Chem. Theory Comput. **15**, 5221 (2019).

[31] J. Hermann, Z. Schätzle, and F. Noé, Nat. Chem. **12**, 891 (2020).

[32] D. Pfau, J. S. Spencer, A. G. D. G. Matthews, and W. M. C. Foulkes, Phys. Rev. Research **2**, 033429 (2020).

[33] R. Jastrow, Phys. Rev. **98**, 1479 (1955).

[34] T. Kato, Commun. Pure Appl. Math. **10**, 151 (1957).

[35] M. G. Endres, D. B. Kaplan, J.-W. Lee, and A. N. Nicholson, Phys. Rev. Lett. **107**, 201601 (2011).

[36] R. M. Martin, L. Reining, and D. M. Ceperley, *Interacting Electrons: Theory and Computational Approaches* (Cambridge University Press, Cambridge, 2016).

[37] P. Giannozzi, S. Baroni, N. Bonini, M. Calandra, R. Car, C. Cavazzoni, D. Ceresoli, G. L. Chiarotti, M. Cococcioni, I. Dabo, A. Dal Corso, S. de Gironcoli, S. Fabris, G. Fratesi, R. Gebauer, U. Gerstmann, C. Gougoussis, A. Kokalj, M. Lazzeri, L. Martin-Samos, N. Marzari, F. Mauri, R. Mazzarello, S. Paolini, A. Pasquarello, L. Paulatto, C. Sbraccia, S. Scandolo, G. Sclauzero, A. P. Seitsonen, A. Smogunov, P. Umari, and R. M. Wentzcovitch, J. Phys.: Condens. Matter **21**, 395502 (2009).

[38] J. T. Krogel, J. A. Santana, and F. A. Reboredo, Phys. Rev. B **93**, 075143 (2016).

[39] J. P. Perdew, K. Burke, and M. Ernzerhof, Phys. Rev. Lett. **77**, 3865 (1996).

[40] J. Kim, A. Baczewski, T. Beaudet, A. Benali, C. Bennett, M. Berrill, N. Blunt, E. J. L. Borda, M. Casula, D. Ceperley, S. Chiesa, B. K. Clark, R. Clay, K. Delaney, M. Dewing, K. Esler, H. Hao, O. Heinonen, P. R. C. Kent, J. T. Krogel, I. Kylanpaa, Y. W. Li, M. G. Lopez, Y. Luo, F. Malone, R. Martin, A. Mathuriya, J. McMinis, C. Melton, L. Mitas, M. A. Morales, E. Neuscamman, W. Parker, S. Flores, N. A. Romero, B. Rubenstein, J. Shea, H. Shin, L. Shulenburger, A. Tillack, J. Townsend, N. Tubman, B. van der Goetz, J. Vincent, D. C.

Yang, Y. Yang, S. Zhang, and L. Zhao, J. Phys.: Condens. Matter **30**, 195901 (2018).

[41] L. Zhao and E. Neuscamman, J. Chem. Theory Comput. **13**, 2604 (2017).

[42] K. Esler, J. Kim, D. Ceperley, and L. Shulenburger, Comput. Sci. Eng. **14**, 40 (2012).

[43] Y. Luo, K. P. Esler, P. R. C. Kent, and L. Shulenburger, J. Chem. Phys. **149**, 084107 (2018).

[44] M. Holzmann, B. Bernu, and D. M. Ceperley, Phys. Rev. B **74**, 104510 (2006).

[45] P. Battle and A. Cheetham, J. Phys. C **12**, 337 (1979).

[46] H. Fjellvåg, F. Grønvold, S. Stølen, and B. Hauback, J. Solid State Chem. **124**, 52 (1996).

[47] J. Kanamori, J. Appl. Phys. **31**, S14 (1960).

[48] P. W. Anderson, Phys. Rev. **79**, 350 (1950).

[49] N. Trivedi and D. M. Ceperley, Phys. Rev. B **41**, 4552 (1990).

[50] G. Trimarchi, Z. Wang, and A. Zunger, Polymorphous band structure model of gapping in the antiferromagnetic and paramagnetic phases of the Mott insulators MnO, FeO, CoO, and NiO, Phys. Rev. B **97**, 035107 (2018).

[51] J. P. Townsend, S. D. Pineda Flores, R. C. Clay III, T. R. Mattsson, E. Neuscamman, L. Zhao, R. E. Cohen, and L. Shulenburger, dataset for "Starting-point independent quantum Monte Carlo calculations of iron oxide", 2020, doi: 10.18126/nur5-90xb.

[52] www.gausscentre.eu.

[53] www.lrz.de.